



ЕКСПЕРИМЕНТАЛНА И НУМЕРИЧКА АНАЛИЗА ЈЕДНОСТАВНОГ МОДЕЛА РАМОВСКЕ КОНСТРУКЦИЈЕ СА ПРИГУШИВАЧЕМ СА УСКЛАЂЕНИМ КРЕТАЊЕМ ВОДЕ

Mladen Šiljegović, *Gaisc@yahoo.com*,

University of Banja Luka, Faculty of Architecture, Civil Engineering and Geodesy;

Marina Latinović, *mar.latinovic@gmail.com*, IUGERS - Institute for Urbanism, Civil
engineering and Ecology of Republic of Srpska, Banja Luka

Ognjen Mijatović, *mijatovicognjennada@gmail.com*,

Derby Design Engineering, Dubai

Aleksandar Borkovic, *aleksandar.borkovic@aggf.unibl.org*,

University of Banja Luka, Faculty of Architecture, Civil Engineering and Geodesy

Valentina Golubović-Bugarški, *valentina.golubovic-bugarški@mf.unibl.org*,

University of Banja Luka, Faculty of Mechanical Engineering

Резиме:

У овом раду је укратко дат осврт на врсте, принципе рада и анализе система за пригушивање вибрација инжењерских конструкција, са акцентом на усклађеним пригушивачима. Изложени су резултати експерименталне и нумеричке анализе алуминијумске скелетне конструкције побуђене заданим почетним помјерањем. Динамички параметри (сопствене фреквенције и пригушења), добијени мјерењима на основном експерименталном моделу, поређени су са нумеричким моделом, а затим су вршена међусобна поређења параметара различитих варијанти експерименталног модела. Анализирани су и упоређени одговори модела са и без система за пригушивање. Као пригушивач је кориштена посуда са водом постављена на врх конструкције. Вариран је ниво воде у посуди, као и положај резервоара у односу на правац побуде. За све варијанте модела, приказане су вриједности прве и друге сопствене фреквенције у правцу побуђивања те су процијењене вриједности пригушења.

Кључне ријечи: експериментална динамичка анализа, пригушење, усклађено кретање воде

EXPERIMENTAL AND NUMERICAL ANALYSIS OF A SIMPLE FRAME STRUCTURAL MODEL WITH TUNED LIQUID DAMPER

Abstract:

In this paper, a brief overview of damping systems and their operation and analysis principles is provided, with emphasis on tuned damping systems of engineering structures. The results of the experimental analysis are presented for an aluminum frame structure excited with initial displacement. The measured dynamic parameters (eigenfrequencies and dumping factors) of the basic experimental model are compared with the numerical model values. Furthermore, the comparison of the results obtained for

different variants of the experimental model are shown. Responses of models with and without the damping device are considered. A water reservoir placed on top of the structure is utilized as a damping device. The water level in the reservoir and orientation of the reservoir with respect to the direction of excitation force are varied. For all model variants, the values of the first and the second eigenfrequencies in the direction of excitation are shown and the corresponding damping values are estimated.

Keywords: experimental dynamic analysis, damping, tuned liquid movements

1. INTRODUCTION

Contemporary skyscrapers are extremely flexible structures whose dynamic analysis is of extreme importance. The swaying of a building can be disturbing for inhabitants and many devices are introduced to diminish its effect. These devices are called dampers and their main purpose is to control earthquake and wind-induced vibrations in buildings. However, they can meliorate the behavior of the building in response to other types of dynamic excitations, too.

Earthquakes can cause excessive random oscillations for many types of buildings. Nevertheless, the wind, in some regions, is a dominant load for the design of flexible high-rise buildings because of their high oscillation period.

The influence of the damper on structural response is often analyzed in literature. One of the most comprehensive research is given by Koščak and Turkalj in [1]. They experimentally analyzed the dynamical characteristics of a multistory frame structure model and compared it with a numerical model. Additionally, the influence of a water reservoir and pendulum with corresponding mass is examined.

Also, a study of tuned liquid mass dampers performance test is given in [2]. Authors of this study focused on reduction of a bi-directional response of a building. Firstly, they tested a small-scale model of tuned liquid mass dampers using a shaking table. By changing direction of a damper, relative to the direction of excitation, they simulated behavior of a tuned liquid column damper and a tuned mass damper. After detail analysis of obtained results, they manufactured a full-scale damper and performed testing on a five story steel building. Interesting study is given in [3], where authors developed a 3.7-ton transmission system with one degree of freedom. It had adjustable dynamic characteristics in order to simulate structures natural frequencies between 0.7 and 2 Hz and to validate tuned liquid dampers' properties.

The paper is organized as follows. Next section deals with some basic concepts of structural damping devices. The third section gives brief description of physical and numerical model and it is followed by concise explanation of experiment setup. Results and discussion are given in fifth section, while the conclusions are made at the end section.

2. STRUCTURAL DAMPERS

When structural damping devices are considered, we can distinguish passive damping devices and tuned systems. Passive damping devices include metallic, friction, viscous and viscoelastic dampers. Tuned systems include mass dampers and they are also called tuned dampers because the natural frequencies of these devices are tuned to be equal or similar to the natural frequencies of the structure to which they are attached. Herein, the focus is on this type of dampers, but few words are also given about passive damping devices.

Friction dampers are devices for which the accumulated energy is spent on overcoming friction at the contact surfaces, Fig. 1a. In metallic dampers, energy is spent on inelastic deformation of components, Fig. 1b. For passive visco-elastic dampers, materials used are usually polymers that dissipate energy by shear strain. An example is displayed on the Fig. 1c, where the visco-elastic material is located between steel plates. The relative displacement of the outer plates in relation to the center plate results in a dissipation of energy in the layer of highly elastic material. Dry or visco-elastic friction-

based dampers use solid body properties to dissipate energy, but fluids can also be used. When fluids are utilized, dissipation depends on the viscosity of the fluid – viscous pot dampers, or density of the fluid – viscous orifice dampers, Fig. 1d, [4].

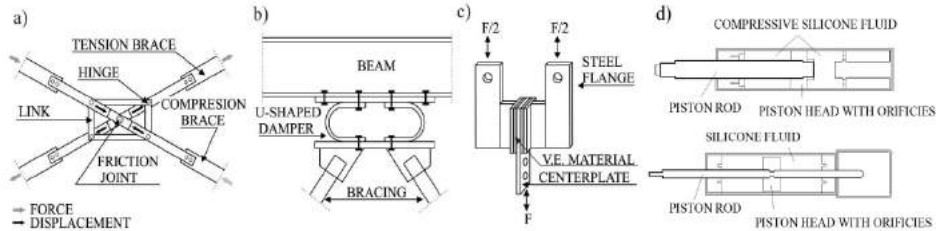


Figure 1. a) Friction damper, b) Metallic damper, c) Viscoelastic damper, d) Viscous pot and orifice damper

Unlike passive damping devices that are placed on structural elements in order to dissipate energy, tuned dampers are devices that must be allowed to move with respect to the building. There are various types of tuned dampers: tuned mass dampers (TMD), tuned liquid dampers (TLD) in containers or tuned liquid dampers with liquid in column, Fig. 2.

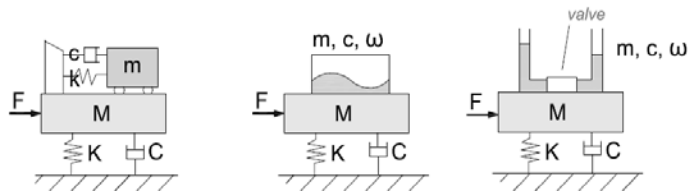


Figure 2. Tuned mass damper, tuned liquid dampers with liquid in a container and in a column

If we consider oscillator with one degree of freedom, subjected to harmonic force, the response of this oscillator may be reduced in amplitude by adding a secondary mass that has a relative movement with respect to the primary oscillator. This added mass is connected to the construction by a spring, or in a form of pendulum, and by a damper, Fig. 3a.

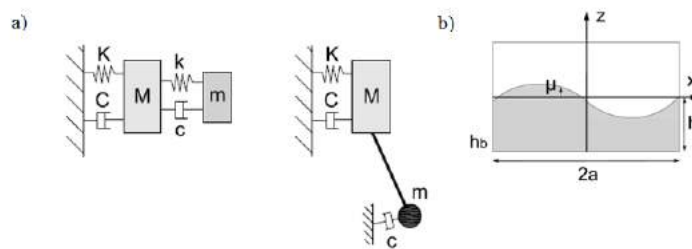


Figure 3. a) Tuned mass dampers with a spring or pendulum b) Schema of container filled with water

When construction vibrates, it excites the damper mass simultaneously. The kinetic energy transferred from the structure to the TMD gets absorbed by a damping component of the device.

Relative displacement of the primary oscillator with respect to the TMD can be described by following equations [5]:

$$M\ddot{y}_1(t) + C_1\dot{y}_1(t) + Ky_1(t) = c\dot{y}_2(t) + ky_2(t) + f(t) \quad (1)$$

$$m\ddot{y}_2(t) + c\dot{y}_2(t) + ky_2(t) = -m\ddot{y}_1(t) \quad (2)$$

Analysis of these equations enables sizing (tuning) of a mass damper in order to get maximum damping. Since added mass introduces another degree of freedom in construction, in diagram of movement/frequency two peaks are seen, where without damping mass there was only one peak. The minimum amplitude of the resonance is thus obtained by choosing the optimum tuning, mass and damping ratio. Tuning ratio is defined as ratio of fundamental frequency of construction to the one of damper. Mass ratio relates masses of a damper and construction. [6]

Recently, a new system that consists of multiple mass dampers (MMD) is in use. These devices can be more efficient than TMD, because they can be adjusted to damp much wider frequency spectrum. [5]

Another category of mass dampers consists of replacing a mass and a damper by a container filled with liquid. In this case, the liquid is the secondary mass, and the damping is provided by a friction between the liquid and the container walls - sloshing effect. The most often utilized liquid is water.

In fluid dynamics, slosh refers to the movement of a liquid inside another oscillating object. When container starts to oscillate, waves on the water surface move to different directions due to fluid inertia. Energy needed for moving of the wave diminishes the oscillation energy of construction, which reduces the amplitude of oscillation. Standing wave induced in this manner has its own frequency, which is a function of water depth and container shape, [1]. For rectangular container, according to the linear theory of the boundary layer, frequencies of natural modes can be determined by the equation:

$$f_n = \frac{\omega_n}{2\pi} = \sqrt{\frac{2n-1}{2a} \pi g \tanh \frac{\pi h}{2a}} \quad (3)$$

where ω_n is circular frequency of mode n , a is length of container in the direction of oscillation, g gravity acceleration, and h is depth of water in container. For $n=1$, natural frequency of the first mode is obtained and this mode has dominant effect in relation to the other modes. Therefore, TLD is designed in such a way that the frequency of the first mode of water surface oscillation is close to the first frequency of considered structure, [1]. In case of a column liquid damper, the vibration frequency is $\sqrt{2g/l}$, where l is column length. [6]

Liquid in container can be modeled with multiple masses, where one of them is connected to container walls by rigid connection, while the others are connected with springs. This shows analogy that can be established between a TMD and a TLD. Equations of this system can be written in exactly the same way as equations (1) and (2), with $m = \rho 2bh$, $c = 2m\xi\omega$, $k = m\omega^2$. [5]

The principle used for sizing of the TMD can also be applied to TLD. Although the parameters of a TMD can be optimized and analytical solution provided, the nonlinear response of the moving fluid in a container makes such optimization very difficult.

Behavior of TLD can be modeled by equivalent linear elastic system, when vibration amplitudes are small. Because the damping ratio of water is small, 1-5 %, approximation with linear model is feasible. When vibration amplitudes are large, TLD behavior becomes nonlinear and parameters k and c become nonlinear, too. For equivalent TMD, they are determined experimentally. [2]

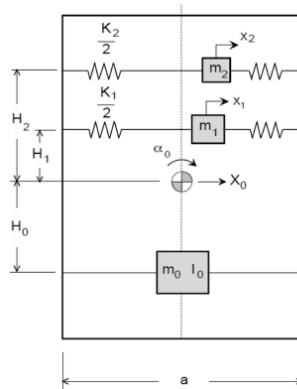


Figure 4. Equivalent mechanical model of a TLD [2]

3. PHYSICAL AND NUMERICAL MODEL

3.1. PHYSICAL MODEL



Figure 5. Experimental setup

For physical model, main structural material is aluminum, which is more favorable than structural steel due to two reasons. It is more convenient for crafting while the lower modulus of elasticity results with more flexible structure. Floor slabs are made with plywood with additional stainless-steel sheets bolted on the lower side of the slab. Foundation structure is made of steel.

Besides the main model, additional structure with purpose of application of initial displacement is constructed. It consists of wooden stand and weight.

Construction of static system is considered to ensure that model oscillates in the first mode in XZ plane, and torsional oscillations are avoided in order to simplify analysis of the results.

Disposition and details of basic experimental model are given in Fig. 6. For different variants of model, weights are added on the upper floor as well as plastic container (203x135mm) that served as TLD.

Beams and columns connections are made with one M3 bolt per connection. In direction X, in which the construction is set to vibrate and the measuring of response is made, joint (pin) connections are simulated in a way that nuts are left loose and the beam connection are set free to rotate around the bolt. All connections are lubricated to reduce

friction as much as possible. Thus, free moment connections are achieved in X direction. In Y direction, bolts are tightened with full tightening force. Since the excitation force is relatively weak, beam-columns connections didn't slip or rotate (intensive micro and macro slipping didn't occur) and they remained in linear damping region. This can be seen from acceleration response of the tested construction. Considering all mentioned above, connections in Y direction can be taken as approximately rigid.

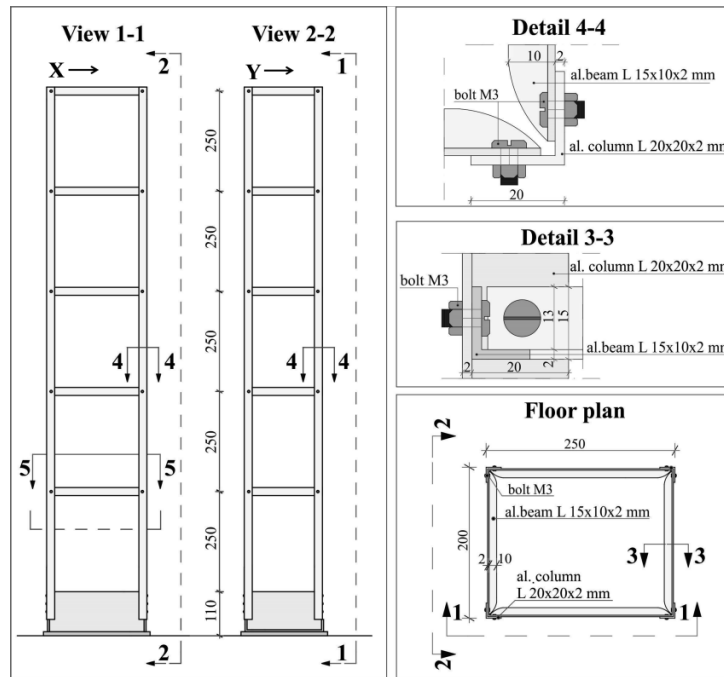


Figure 6. Disposition and characteristic details of physical model

Characteristic of the beam-column connection in X direction could be changed during multiple tests, due to the relatively large displacement of upper floors. This could lead to situation where the model would not remain the same before and after testing. Periods of oscillations before and after the test would be different, which would lead to difficulty in comparing the results. This effect of structure softening after the excitation, where we have different periods of structure oscillation before and after the application of dynamic force is extensively discussed in [7]. In experiment discussed herein, softening can be neglected since the excitation force is relatively small, and in order to set connections, several previous trial tests were performed.

Floor slabs are freely supported on beams placed in X direction, and they do not touch beams along Y direction. In this way, rigidity in X direction is not affected. Besides, plywood floor slabs are much thicker than the rest of the construction, so it is achieved that the floor slabs together with beams placed in X direction can be considered as rigid plates hinged with two frames, Fig 6. This is important because of defining connections in numerical model. Otherwise, the rigidity between floor slabs and truss structure would be unknown.

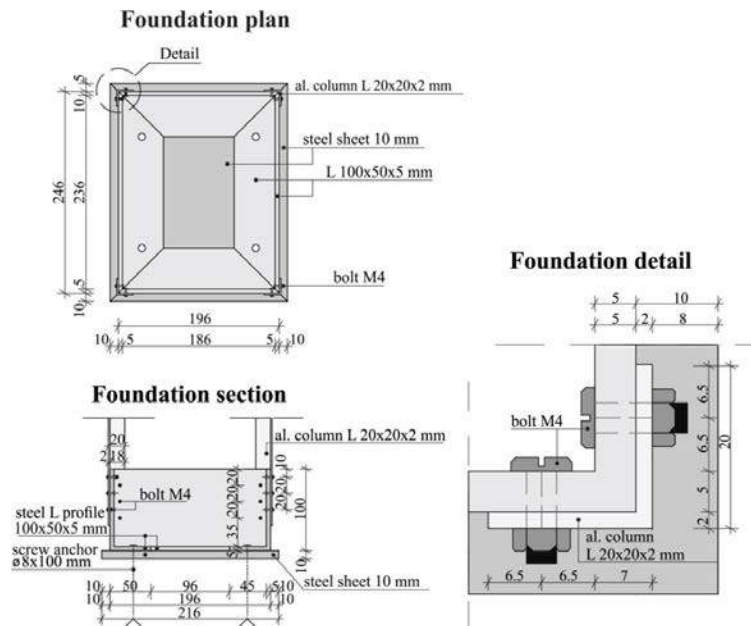


Figure 7. Foundation plan and section, column-foundation connection detail

Model columns are connected on external side of steel foundation structure and joined to it, each with six M4 bolts. Steel foundation is anchored into the concrete floor with four 8 mm diameter anchors, of 100 mm length, Fig. 7. Thus, connections between columns and foundations in numerical model are meant to be considered as full moment connections. After test result analysis and comparison with numerical results, where columns are fully fixed (model variants M0, N2, Table 1), it is concluded that this connection, although made with six bolts for each column, could not be considered as full moment connection. Hence, connections are set as partially rigid in numerical model, concerning bending moment. They are calibrated in a way that numerical model gives results with minimum deviations from experimental results (model variant N1).

Considering above said, tested model can be observed as a vertical console with discontinues rigidity in column connection zone. Dimensions of box profiles of foundation structure are chosen in a way that its rigidity is considerably higher than the truss part of the structure. This minimized its influence on model response.

In experimental results processing, in order to gain damping values, model is seen as one degree of freedom dynamic system.

3.2. NUMERICAL MODEL

Numerical model was made in program SAP2000. Model was made only for basic experimental structure M0, in order to compare the frequency response of experimental and numerical setup, Fig 8.

Two variants of numerical model were made: N1 and N2. N1 variant considers full moment connections of columns restraints, while N2 variant is with a calibrated stiffness of restraints. This calibration is made with respect to the experimentally obtained frequency. Concretely, stiffness of moment connection is modified until the first frequency approximately matched the first frequency obtained in the experiment for base model. Since it is concluded that floors have no influence on the rigidity of construction

as a whole in XZ plane, influence of floors mass is distributed evenly in joints of numerical model.

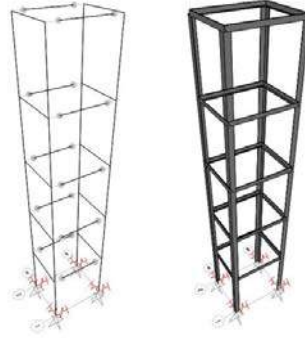


Figure 8. 3D view of numerical model

All variants of physical and numerical models are given in Table 1.

Table 1. Variants of physical and numerical model

Mark	Model variant	Mass (Kg)
M0	Basic model	6.792
M1	330g of added mass on the upper floor	7.122
M2	660g of added mass on the upper floor	7.452
M3	990g of added mass on the upper floor	7.782
M4	1320g of added mass on the upper floor	8.112
V1P1	135mm water tank in 'X' direction Mass of water and the tank combined is 330g	7.122
V2P1	135mm water tank in 'X' direction Mass of water and the tank combined is 660g	7.452
V3P1	135mm water tank in 'X' direction Mass of water and the tank combined is 990g	7.782
V4P1	135mm water tank in 'X' direction Mass of water and the tank combined is 1320g	8.112
V2P2	203mm water tank in 'X' direction Mass of water and the tank combined is 660g	7.452
V3P2	203mm water tank in 'X' direction Mass of water and the tank combined is 990g	7.782
V4P2	203mm water tank in 'X' direction Mass of water and the tank combined is 1320g	8.112
N1	Numerical model (basic model) – tuned spring restraints	
N2	Numerical model (basic model) – fixed restraints	

4. EXPERIMENT SETUP

4.1. ACQUISITION SYSTEM

Free decay responses of vibration were measured using the four-channel acquisition system Portable Pulse of type 3560C, manufactured by Bruel&Kjaer and accelerometer,

of type 4570, also made by Bruel&Kjaer. The root mean square (r.m.s.) values of structure acceleration response were measured using the Fast Fourier Transform (FFT) analyzer integrated into the acquisition system Portable Pulse.

The FFT analyzer set-up was as follows:

- the frequency span: 0-25 Hz
- number of measured lines: 200
- the frequency resolution: 0.125 Hz;
- number of linear averaging of r.m.s. values of acceleration amplitude: 10.

Time-response functions and autospectrum functions were recorded in the Data Recorder of the Pulse LabShop software.

4.2. EXPERIMENT COURSE

Experimental tests consisted of multiple acceleration measurements, with an accelerometer placed on the top of the structure. Excitation mechanism is shown in Fig. 9. The response is measured on basic model, model with additional stationary mass added on the top floor, and model with water reservoir on top, with dimensions 135x203 mm. Detail description of model variations is given in Table 1. For each variant, results from three measurements are obtained, and then averaged.

Accelerometer is placed on the middle of the beam in Y direction, on the top of the model, so it could measure excitations along X direction. For each measurement, the excitation was induced by placing the weight of 1042 g, suspended by the rope fastened at the structure's upper floor. Weight forced the structure to take new equilibrium position, and after the rope that held the weight was cut, the structure started to vibrate.

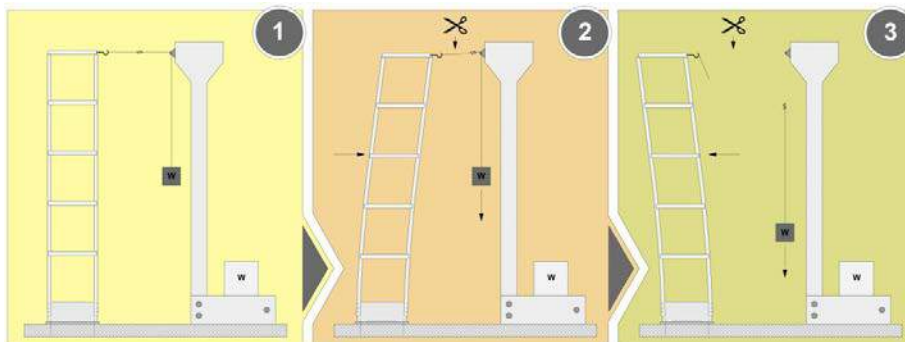


Figure 9. Model excitation scheme

5. RESULTS AND DISCUSSION

5.1. EIGENFREQUENCIES

Eigenfrequencies of tested model are determined by processing data obtained from accelerometer and data acquisition equipment, using Microsoft Excel. Results are shown in a form of graphs. By spotting characteristic peak on graph, and reading its abscissa value, dominant frequency is obtained. It is the frequency of the first eigenmode.

Also, it is possible to note the second eigenfrequency in XZ plane, Fig 10. Regarding data obtained from models which contained reservoir with high level of water, eigenfrequencies of oscillating water can also be noted, Fig 10.

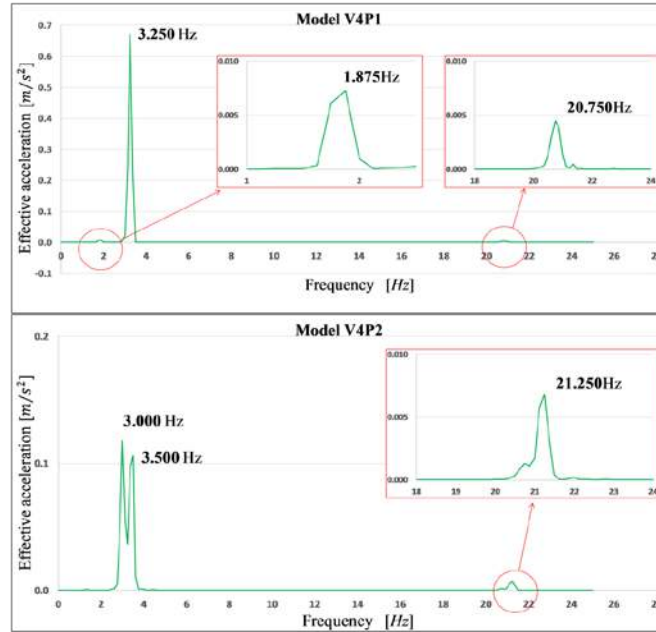


Figure 10. Eigenfrequencies determination, models V4P1 and V4P2

Frequencies obtained experimentally, for all model variations, and also their averaged values, are given in Tab. 2.

The lowest three eigenfrequencies of oscillating water are calculated using the expression (3) and these values can be compared with the experimental results. Calculated values are given in Tab. 3.

Table 2. Experimentally obtained eigenfrequencies of all model variations

Model mark	1st natural frequency, XZ plane f[Hz]				2nd natural frequency, XZ plane f[Hz]				
	Measurement number			Average	Measurement number			Average	
	1	2	3		1	2	3		
Experimental	M0	3.375	3.375	3.375	3.375	21.750	21.750	21.750	21.750
	M1	3.125	3.125	3.125	3.125	21.125	21.125	21.125	21.125
	M2	3.000	3.000	3.000	3.000	20.750	20.750	20.625	20.588
	M3	2.875	2.875	2.875	2.875	20.375	20.375	20.375	20.375
	M4	2.750	2.750	2.875	2.792	20.000	20.250	20.000	20.083
	V1P1	3.250	3.250	3.250	3.250	21.375	21.375	21.375	21.375
	V2P1	3.250	3.250	3.250	3.250	21.250	21.250	21.250	21.250
	V3P1	3.250	3.250	3.250	3.250	21.000	21.000	21.000	21.000
	V4P1	3.250	3.250	3.250	3.250	20.750	20.875	20.750	20.792
	V2P2	3.250	3.375	3.250	3.292	21.375	21.375	21.250	21.333
Experimental	*V3P2	3.375	3.375	3.375	3.375	21.375	21.375	21.375	21.375
	*V4P2	3.000	3.000	3.000	3.000	21.250	21.250	21.250	21.250
Numerical	N1	/	/	/	3.375	/	/	/	20.007
	N2	/	/	/	3.654	/	/	/	23.614

Table 3. Calculated natural frequencies of water depending on tank length and water depth

Model mark	Water tank length l[mm]	Water depth h[mm]	Natural frequency f[Hz]		
			1	2	3
V1P1	135	5	0.826	1.432	1.848
V2P1	135	17	1.483	2.568	3.315
V3P1	135	29	1.849	3.202	4.134
V4P1	135	41	2.073	3.591	4.637
V2P2	203	17	1.001	1.732	2.236
V3P2	203	29	1.276	2.210	2.853
V4P2	203	41	1.471	2.549	3.291

5.2. DAMPING

By experimental measurements, using accelerometer and data acquisition software, accelerations of model top in time domain and along X direction are obtained. Graphical representation of these accelerations is processed in Microsoft Excel. Envelope is obtained following equations of a system with one DOF. The equation of motion of free damped vibrations of this system, for damping less than the critical, is as follows:

$$y = Ce^{-\xi\omega t}\sin(\omega_d t) \quad (4)$$

where the phase angle equals zero.

Acceleration is obtained after derivation of this equation with respect to time:

$$\ddot{y} = Ce^{-\xi\omega t}[\xi^2\omega^2\sin(\omega_d t) - 2\xi\omega\cos(\omega_d t)\omega_d - \sin(\omega_d t)\omega_d^2] \quad (5)$$

Terms $\xi^2\omega^2\sin(\omega_d t)$ and $2\xi\omega\cos(\omega_d t)\omega_d$ can be neglected, because they do not affect result significantly, and also damping estimation is much easier. After neglecting these two terms the equation remained is following:

$$\ddot{y} = Ce^{-\xi\omega t}[-\sin(\omega_d t)\omega_d^2] \quad (6)$$

For $\sin(\omega_d t) = \pm 1$ envelopes are obtained:

$$\dot{y} = -Ce^{-\xi\omega t}\omega_d^2, \quad \dot{y} = Ce^{-\xi\omega t}\omega_d^2 \quad (7)$$

Unknown values are initial amplitude C and damping ratio ξ . By varying these values and harmonization of envelope with acceleration graph, calibrated estimated values of initial amplitude and damping factor are obtained, Fig. 11.

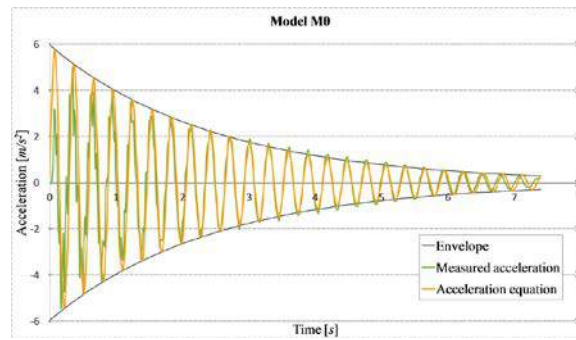


Figure 11. Model M0 response compared to acceleration equation and its envelopes

Estimated values of initial amplitude and damping are given in Table 4, where asterisk denotes models for which damping cannot be precisely estimated due to beating.

Graphical presentation of individual responses with envelopes, regarding different variants of model are given on Fig. 12.

Table 4. Estimated values of initial amplitude and damping for all model variants

Model mark	First amplitude C[m]				Damping ξ			
	Measurement number			Average	Measurement number			Average
	1	2	3		1	2	3	
M0	0.013	0.012	0.013	0.0127	0.0190	0.0185	0.0190	0.0188
M1	0.013	0.013	0.012	0.0127	0.0190	0.0185	0.0190	0.0188
M2	0.011	0.011	0.011	0.0110	0.0180	0.0175	0.0170	0.0175
M3	0.011	0.011	0.011	0.0110	0.0175	0.0175	0.0175	0.0175
M4	0.011	0.012	0.011	0.0113	0.0185	0.0175	0.0170	0.0177
V1P1	0.012	0.013	0.014	0.0130	0.0270	0.0280	0.0270	0.0273
V2P1	0.011	0.011	0.010	0.0107	0.0240	0.0240	0.0230	0.0237
V3P1	0.010	0.010	0.012	0.0105	0.0210	0.0220	0.0230	0.0220
V4P1	0.010	0.009	0.010	0.0097	0.0200	0.0210	0.0210	0.0207
V2P2	0.012	0.012	0.012	0.0120	0.0390	0.0370	0.0380	0.0380
*V3P2	0.010	0.010	0.011	0.0103	0.0320	0.0300	0.0310	0.0310
*V4P2	0.011	0.011	0.011	0.0110	0.0260	0.0260	0.0260	0.0260

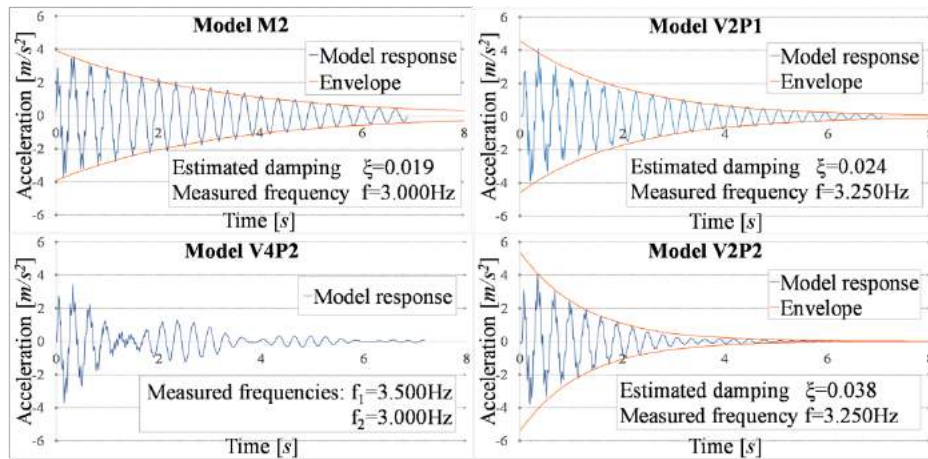


Figure 12. Examples of model responses with envelopes

5.3. DISCUSSION

Obtained results enable comparison of different model variations responses:

- Models with no damping device and different mass on top: M0, M1, M2, M3, M4;
- Models with the same mass with and without damping device: M2, V2P1, V2P2; M3, V3P1, V3P2;
- Models with TLD with different water levels: V1P1, V2P1, V3P1, V4P1; V2P2, V3P2, V4P2;
- Basic physical and numerical models: M0, N1.

Based on the comparison of the results obtained on model without damper, with different masses on the highest level, it is concluded that the frequencies of oscillations decrease when mass increases, which is expected. Additionally, it can be concluded that the added mass on the highest level of the model does not have much impact on the change of damping, Fig. 13, Tab. 5.

Table 5. Comparison of eigenfrequencies and estimated damping (Fig. 13, Fig.14)

Model mark	Average frequency f [Hz]	Δf (%)	Average damping ξ	$\Delta \xi$ (%)
M0	3.375	/	0.0188	/
M2	3.000	-11.11	0.0175	-6.91
M4	2.792	-17.27	0.0177	-5.85
Δf (%); $\Delta \xi$ (%) expressed relative to M0				
M2	3.000	/	0.0175	/
V2P1	3.250	8.33	0.0237	35.43
V2P2	3.292	9.73	0.0380	117.14
Δf (%); $\Delta \xi$ (%) expressed relative to M2				
M3	2.875	/	0.0175	/
V3P1	3.250	13.04	0.0220	25.71
V3P2	3.375	17.39	0.0310	77.14
Δf (%); $\Delta \xi$ (%) expressed relative to M3				

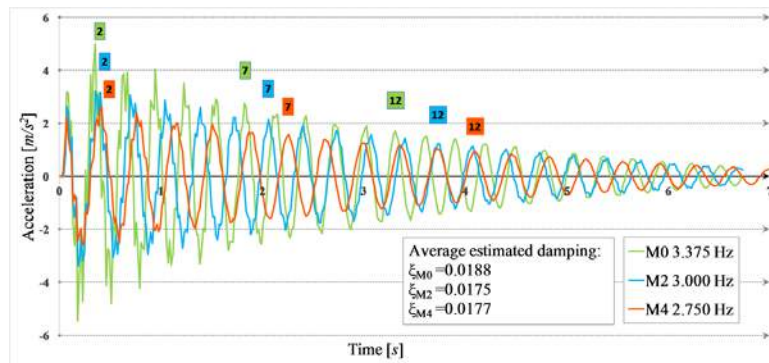


Figure 13. Response comparison, models M0, M2, M4

By comparison of responses of the models with the same mass, with and without a damper, it can be concluded that the water reservoir significantly increases damping. Model with the reservoir set in direction 2 (P2, reservoir length 203 mm) gave higher damping values than the ones when a reservoir is placed in direction 1 (P1, reservoir length 135 mm), Tab 6, Fig 15. Reason for this difference in model responses we can seek in oscillation synchronization of active (moved) part of liquid in reservoir and oscillation of model. In second direction beating phenomenon is observed. Its influence can be related with higher damping values. Beating is phenomena which occurs when two oscillations of the same amplitude interact creating specific pattern [8], [9].

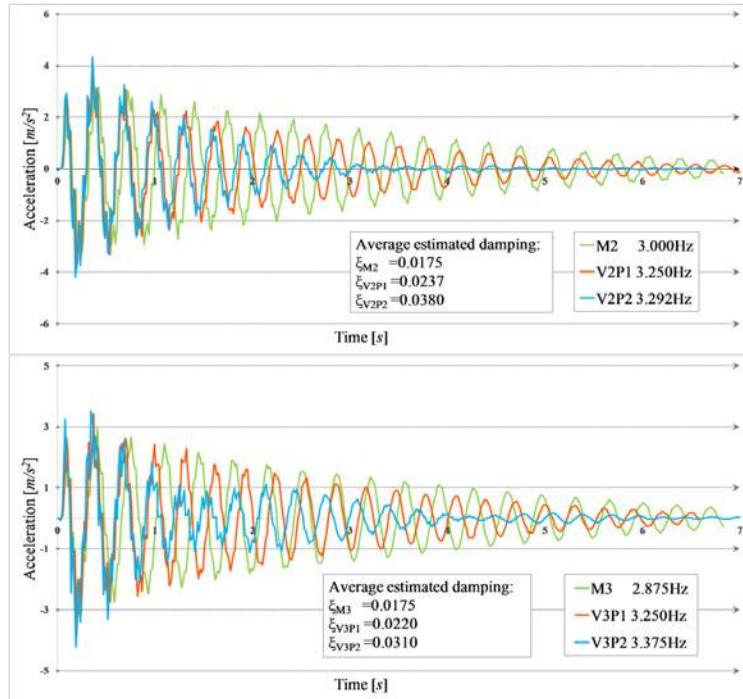


Figure 14. Acceleration response comparisons

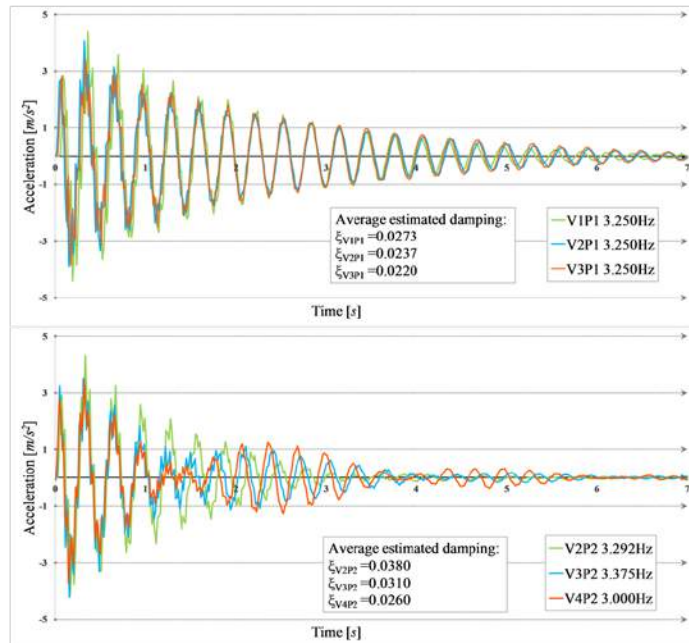


Figure 15. Acceleration response comparisons

Table 6. Comparison of eigenfrequencies and estimated damping (Fig. 15)

Model mark	Average frequency f[Hz]	Δf (%)	Average damping ξ	$\Delta \xi$ (%)
V1P1	3.250	/	0.0273	/
V2P1	3.250	0.00	0.0237	-13.19
V3P1	3.250	0.00	0.0220	-19.41
Δf (%); $\Delta \xi$ (%) expressed relative to V1P1				
V2P2	3.292	/	0.0380	/
V3P2	3.375	-2.52	0.0310	-18.42
V4P2	3.000	-8.87	0.0260	-31.58
Δf (%); $\Delta \xi$ (%) expressed relative to V2P2				

By the increase of the water level in the reservoir, damping factor decreases. With higher water level, the influence of water mass which stays still is greater, and this still water acts as mass attached to the system. This mass does not affect damping factor, so it is expected that damping decreases when water level rises, Fig. 15, Tab. 6.

On models V3P2 and V4P2 beating is obvious, Fig 15, which is clearly indicated on graphical representations of model responses. Most obvious beating is on model V4P2. Since water mass in reservoir is significant in comparison to model mass (water mass in reservoir is 1,132 kg, and the mass of total model is 6,792 kg) amplitude ratio is approximately equal, and beating is clearly indicated. That is the reason why, for variants V3P2 and V4P2, values of estimated damping and indicated frequency should be taken with uncertainty.

Comparison of accelerations of numerical model N1 and corresponding physical model M0, it can be seen that their responses are slightly out of phase. However, well compliance is achieved, Fig 16. Main reason for this compliance is adjustment of experimental model to avoid the influence of damping in connection joints. This damping can be very significant and it could lead up to 30% differences in experimental and numerical results using wire finite elements, [8]. The influence of the intensity of the perturbation on the construction's response also should not be neglected. In performed experiment, as mentioned earlier, because of the small intensity of the perturbation, there has been no friction activation and slipping into column-beam joints.

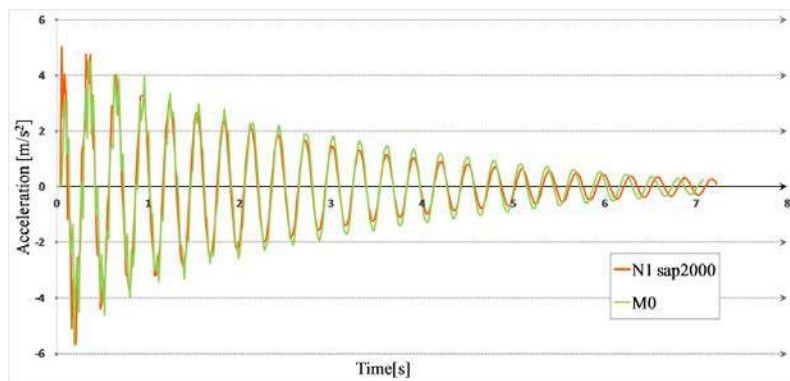


Figure 16. Acceleration response comparisons

6. CONCLUSIONS

TMD is an effective solution for reduction of vibrations induced by dynamic forces. Herein, an influence of TLD on simple frame model is demonstrated. Due to many restrictions, simple model is created using available resources. It is calibrated in such a way that its response can be modeled with one degree of freedom system. Experimental analysis revealed some interesting facts considering changes in frequencies, as well as damping and beating phenomena occurrence. It can be concluded that the highest level of damping occurs when water reservoir is placed longitudinally with respect to excitation direction. This case is also related to the occurrence of beating.

Further research is required in order to draw more firm conclusions. It should consist of testing various TLD, in order to get better tuning between the first eigenfrequency of a model and a damper. Also, it may be useful to try to lower the first mode frequency of the model to match values around 1 Hz, since dominant modes of real buildings are in that range.

LITERATURE

- [1] Koščak J., and G. Turkalj, "Modalna analiza modela konstrukcije i ispitivanje uticaja njihala i spremnika sa vodom kao prigušivača", Sveučilište u Zagrebu, Građevinski fakultet, Zagreb 2012.
- [2] Kyung-Won M., K.. Junhee, and K.. Young-Wook, "Design and test of tuned liquid mass dampers for attenuation of the wind responses of a full scale building", *Smart materials and structures*, vol. 23, no 4, March 2014.
- [3] Silva F. M. J., and A. C. Costa, "Experimental studies on the characteristics of tuned liquid dampers for reducing vibration in structures", *The 14th world conference on earthquake engineering*, Beijing, 2008
- [4] Heysami A, "Types of dampers and their seismic performance during an earthquake", *Current world environment* vol. 10(special issue 1), 2015
- [5] Assessment of vibrational behaviour of footbridges under pedestrian loading, Appendix 3: Damping systems, *Service d'Etudes techniques des routes et autoroutes – Setra*, 2006
- [6] Sadek F., B. Mohraz, A. W. Taylor and R. M. Chung, "Passive energy dissipation devices for seismic application", *National Institute of Standards and Technology*, Nistir5923, 1996
- [7] Taranah B. S., "Reinforced concrete design of tall buildings", Boca Racon: CRC press Taylor and Francis group, 2010.
- [8] Golubović-Bugarski V., O. Mijatović, M. Guzijan-Dilber, M. Desančić and A. Borković, "Identification of dynamic properties of mechanical structures from measured vibration responses", *6th International congress of Serbian society of mechanics*, 2017
- [9] Clough R. and J. Penzien, "Dynamics of structures", *Berekeley: Computers and structures*, 2003.